Contents lists available at SCCE

Journal of Soft Computing in Civil Engineering

Journal homepage: www.jsoftcivil.com

Discrete Sizing Optimization of Steel Structures Using Modified Fireworks Algorithm

Navid Seraji [1]; Mehdi Babaei [2,*]

1. Ph.D. Student, Department of Civil Engineering, Faculty of Engineering, University of Zanjan, Zanjan, Iran
2. Associate Professor, Department of Civil Engineering, Faculty of Engineering, University of Zanjan, Zanjan, Iran
* Corresponding author: *mbabaei@znu.ac.ir*

https://doi.org/10.22115/scce.2024.396409.1642

ARTICLE INFO

Article history:
Received: 08 May 2023
Revised: 13 August 2023
Accepted: 22 January 2024

Keywords:
Fireworks algorithm;
Discrete optimization;
Structural engineering;
Moment-resisting frames;
Truss structures.

ABSTRACT

Fireworks algorithm (FWA) is an artificial intelligence algorithm developed by emulating the burst process of fireworks. This paper applies a modified version of fireworks algorithm called MoFWA to design disparate steel trusses and planar frames. In this study, the objective is to improve FWA's performance by adding two operators to it: 1) fly-back mechanism 2) duplicate spark remover operator. Also, its amplitude is changed into a dynamic one to enhance its compatibility with different optimization problems. The function we are focusing on is the total weight of the structure. This takes into account the requirements for serviceability and strength as outlined by the American Institute for Steel Construction's Load and Resistance Factor Design (LRFD) standards. A total of six benchmark structures including a 10-bar truss, a 25-bar truss, a 582-bar tower truss, a two-bay three-story frame, a one-bay 10-story frame, and a three-bay 24-story frame are chosen from previous studies for the optimization. In addition, a comparison is presented between the results of MoFWA with FWA and other optimization methods such as modified sine-cosine algorithm (MSCA), newton meta-heuristic algorithm (NMA), improved grey wolf optimizer (GWOM), enhanced whale optimization algorithm (EWOA), switching teams algorithm (STA), MHBMO, artificial bee colony (ABC), school-based optimization (SBO), teaching-learning based optimization (TLBO), design-driven harmony search (DDHS), and inscribed hyperspheres (IHS). The results indicate that MoFWA is completely better than FWA and can generate superior optimal solutions compared to the other optimization algorithms.

How to cite this article: Seraji N, Babaei M. Discrete sizing optimization of steel structures using modified fireworks algorithm. J Soft Comput Civ Eng 2025;9(1):39–63. https://doi.org/10.22115/scce.2024.396409.1642

2588-2872/ © 2025 The Authors. Published by Pouyan Press.
This is an open access article under the CC BY license (http://creativecommons.org/licenses/by/4.0/).

1. Introduction

Researchers worldwide have grappled with the challenge of structural optimization, and numerous methods and algorithms have been developed to improve various aspects of it. One of the main challenges that researchers are faced with is that most of these algorithms have either significant accuracy with weak computational cost or vice versa. The reason that FWA is chosen in this study is that it has a high potential of outdoing other algorithms. However, it must be noted that FWA has an excessive computational process which is not a favorable characteristic. In this study, we try to modify FWA by adding some new strategies to it and also refining the relationship of its primary amplitude size and coefficients with the size of search space so that it could function better in different circumstances.

When it comes to optimization problems, there are two types: those with one objective and those with multiple objectives, which are known as multi-objective problems. Structural optimization has the primary goal of minimizing the weight of a structure while still meeting the strength and drift constraints specified by code. Our study will focus on discrete variable optimization for steel structures, which we will discuss shortly. For this type of optimization, the design variable selected from steel section tables provided in steel construction manuals is the cross-sectional area of structural members.

There are myriads of meta-heuristic methods for optimal design of engineering problems (e.g., simulated annealing (SA) by [1], teaching–learning based optimization (TLBO) by [2], [3]), ant colony optimization [4], genetic algorithm (GA) by [5,6], particle swarm optimization (PSO) by [7–9], cellular automata (CA) by [10], cuckoo search algorithm (CS) by [11], charged system search (CSS) by [12], Design-driven harmony search (DDHS) by [13], mine blast algorithm (MBA) by [14], artificial bee colony (ABC) by [15], differential evolution (DE) by [16]).

Most of meta-heuristic algorithms are population-based algorithms which means that in each iteration, they produce some probable results that may lead them to the optimal solution. The performance of these algorithms depends on two main features including diversification, and intensification. Also, the interaction between these two has effects on their results. On one hand there is diversification which certifies that all the search space will be covered. In other words, weak diversification leads to poor exploration in search space. In contrast, strong diversification causes getting stuck in local optima which is not a desirable phenomenon. On the other hand, there is intensification that affects the computational process of optimization since it controls the exploitation. The complexity of an optimization problem depends on two factors: 1) search space 2) number of design variables.

The fireworks algorithm (FWA) is a swarm intelligence algorithm that was first introduced by [17]. The FWA is developed by emulating the burst process of fireworks at night. In fireworks algorithm, fireworks are generated randomly all around the search space and each one of them produces a group of sparks all over itself. These fireworks and explosion sparks represent potential solutions for the optimization problem and FWA keeps generating them until a termination criterion is satisfied. One of the main advantages of FWA against other meta-heuristics is its simplicity and capability to easily balance between diversification and

intensification. In contrast, it has some deficiencies such as high computational process and low consideration of the previous solutions. Over the past years, numerous adjustments have been made to the original FWA; for instance, dynFWA by [18], IFWA by [19], FFWA by [20].

In our study, we made some modifications to the FWA (Fireworks Algorithm) by introducing a dynamic amplitude and including two new operators called fly-back mechanism and duplicate spark remover. These changes were aimed at reducing the computational cost of the algorithm while also improving its ability to search for solutions in difficult and marginal areas. Our results show that these modifications are effective and can lead to better performance of the FWA in solving optimization problems.

2. Structural optimization problems

The main objective of structural optimization problems is to minimize the structure weight according to the design variables vector $V = [v_1, v_2, \dots, v_d]$ which contains the section number of structure members for each grouping [21]. The structure weight is calculated as follows:

$$\mathrm{W} = \sum_{\mathrm{i}=1}^{\mathrm{N_m}} \gamma_\mathrm{i} \mathrm{A_i} \mathrm{L_i} \tag{1}$$

Where W is the weight of structure; N_m is the number of members; γ_i is the material density of member i; A_i is the cross-sectional area of member i and L_i is the length of member i.

The original objective is penalized with the following formula:

$$F = W(1 + C)^{\varepsilon} \tag{2}$$

Where ε is a number greater than 1 and C is defined as:

$$C = \sum_{i=1}^{N_m} C_i^{\sigma} + \sum_{i=1}^{N_n} C_i^{\delta} + \sum_{i=1}^{N_c} C_i^{I} \tag{1}$$

Where $C_i^{\sigma}, C_i^{\delta}$ and C_i^{I} are penalty functions for strength constraint violation, drift constraint violation and axial force-bending moment interaction, respectively. N_m, N_n and N_c are the number of members, number of joints and the number of columns, respectively. The C factor is defined as follows:

$$\mathrm{C_i} = \begin{cases} 0 & \text{if } \propto_\mathrm{i} < 0 \\ \propto_\mathrm{i} & \text{if } \propto_\mathrm{i} > 0 \end{cases} \tag{4}$$

Where $\propto_\mathrm{i}$ is calculated separately from strength and drift constraints:

$$\propto_i^{\sigma} = \frac{|\sigma_i|}{|\sigma_i^{a}|} \text{-} 1 \quad , \quad i = 1, \dots, N_m \tag{5}$$

$$\propto_i^{\delta} = \frac{|\delta_i|}{|\delta_i^{a}|} \text{-} 1 \quad , \quad i = 1, \dots, N_\mathrm{n} \tag{6}$$

Where σ_i is the stress in member i and σ_i^a is the allowable stress of member i; δ_i and δ_i^a are the inter-story drift and allowable inter-story drift of joint i;

$\propto_i^I$ is defined as:

$$\text{For } \frac{P_u}{\varphi_c P_n} < 0.2: \quad \propto_i^I = \left[\frac{P_u}{2\varphi_c P_n} + \frac{M_{ux}}{\varphi_b M_{nx}} + \frac{M_{uy}}{\varphi_b M_{ny}}\right] - 1 \leq 0 \qquad i = 1, \dots, N_e \tag{7}$$

$$\text{For } \frac{P_u}{\varphi_c P_n} \geq 0.2: \quad \propto_i^I = \left[\frac{P_u}{\varphi_c P_n} + \frac{8}{9}\left(\frac{M_{ux}}{\varphi_b M_{nx}} + \frac{M_{uy}}{\varphi_b M_{ny}}\right)\right] - 1 \leq 0 \qquad i = 1, \dots, N_e \tag{8}$$

Where φ_c is the resistance factor ($\varphi_c = 0.9$ for tension, $\varphi_c = 0.85$ for compression); φ_b is the flexural resistance reduction factor ($\varphi_b = 0.9$); M_{ux} and M_{uy} are the required flexural strengths in the x and y directions, respectively; M_{nx} and M_{ny} are the nominal flexural strengths in the x and y directions, respectively; P_u is the required strength; and P_n denotes the nominal strength.

3. Fireworks algorithm

As previously mentioned, the Fireworks algorithm (FWA), was originally presented in a study by Tan and Zhu named Fireworks Algorithm for Optimization 2010. During the past decade, a myriad of researchers have proposed different versions of FWA and it is being used on different branches of optimization such as spam detection, image recognition, digital filter design, and power loss minimization.

A brief explanation of how the FWA algorithm works: First N locations are selected for N fireworks to explode, then each one of them produces a group of explosion sparks around itself, then the fitness values of both fireworks and explosion sparks are evaluated and the best location is chosen to follow the next iteration, this process is continued until a termination criterion is met. When a firework is well manufactured, it has plenty of explosion sparks within a small range around it. In contrast, a bad firework is the one with a few explosion sparks within a large radius. These two features are implemented in the FWA algorithm such that the firework in the best location is the good one while the others are categorized in the bad fireworks group depending on their fitness value.

3.1. Number of sparks

Suppose the FWA is designed for the general optimization problem:

$$\text{Minimize } f(x) \in \mathrm{R}, \quad x_{min} \leq x \leq x_{max} \tag{9}$$

Where $x = [x_1, x_2, \dots, x_d]$ implies a location in potential space, d is the dimension of design variable, *f(x)* is the objective function, and x_{min} and x_{max} refer to the boundary of the potential space. The number of sparks generated by each firework x_i is calculated as follows:

$$s_i = M_e \frac{y_{max} - f(X_i) + \varepsilon}{\sum_{i=1}^{N}(y_{max} - f(X_i)) + \varepsilon} \tag{10}$$

Where $y_{max} = \max\big(f(x_i)\big)$ is the maximum amount of objective function among N fireworks, M_e is a constant amount to control the number of explosion sparks, and ε is utilized to avoid zero-division-error.

Also s_i is limited to two boundaries as follows:

$$\hat{s}_i = \begin{cases} \text{round}(a \cdot m) & \text{if } s_i < am \\ \text{round}(b \cdot m) & \text{if } s_i > bm \ , a < b < 1 \\ \text{round}(s_i) & \text{otherwise} \end{cases} \quad (11)$$

Where a and b are constant parameters to control the boundaries.

3.2. Amplitude of explosion

The amplitude of a well generated firework explosion is smaller than a bad one and it has more sparks. The amplitude of explosion for each firework is defined as follows:

$$A_i = \hat{A}\frac{f(X_i) - y_{min} + \varepsilon}{\sum_{i=1}^{N}(f(X_i) - y_{min}) + \varepsilon} \quad (12)$$

Where $y_{min} = \min\big(f(x_i)\big)$ is the minimum (best) value of objective function among the N fireworks, $\hat{A}$ is a constant for controlling the explosion amplitude.

3.3. Explosion sparks operator

Each firework generates s_i explosion sparks around its current location. Fireworks with better fitness can produce a larger population of explosion sparks within smaller explosion amplitude. For each explosion spark, Algorithm 1 is performed as follows:

Algorithm 1. Spark locationing.

Algorithm
1: Initialization (locationing of the spark) $\tilde{x}_j = x_i$;
2: $z = round\big(d.rand(0,1)\big)$;
3: Random selection z dimensions of $\tilde{x}_j$;
4: Displacement calculation: h=$A_i \times rand(-1,1)$;
5: **for** each dimension $\tilde{x}_k^j \in \{\text{pre} - \text{selected } z \ dimensions \ of \ \tilde{x}_j\}$ **do**
6: $\tilde{x}_k^j = \tilde{x}_k^j$ +h
7: **if** $\tilde{x}_k^j$ out of bounds **then**
8: map $\tilde{x}_k^j$ to the potential space: $\tilde{x}_k^j = x_k^{min} + \big|\tilde{x}_k^j\big|\%\big(x_k^{max} - x_k^{min}\big)$;
9: **end if**
10: **end for**

Where d is the dimension of location x.

An additional way of generating sparks is shown in Algorithm 2:

Algorithm 2. A specific spark locationing.

Algorithm
1: Initialization of the spark location $\tilde{x}_j = x_i$;
2: $z = round\left(d.rand(0,1)\right)$;
3: Random seceltion z dimensions of $\tilde{x}_j$;
4: Calculation of Gaussian explosion coefficient: g = *Gaussian* (1, 1);
5: **for** each dimension $\tilde{x}_k^j \in \{\text{pre} - \text{selected } z \; dimensions \; of \; \tilde{x}_j\}$ **do**
6: $\tilde{x}_k^j = \tilde{x}_k^j . g$;
7: **if** $\tilde{x}_k^j$ out of bounds **then**
8: map $\tilde{x}_k^j$ to the potential space: $\tilde{x}_k^j = \mathrm{x}_\mathrm{k}^{\min} + \left\lvert\tilde{x}_k^j\right\rvert \% \left(\mathrm{x}_\mathrm{k}^{\max} - \mathrm{x}_\mathrm{k}^{\min}\right)$;
9: **end if**
10: **end for**

3.4. Selection of locations

In the FWA algorithm, the location with the highest fitness value is retained as a reference for the subsequent generation. Following that, n-1 locations are chosen according to their distance in order to maintain a diverse range of solutions.

3.5. Dynamic fireworks algorithm

One of the improvements that have been made to FWA is called dynFWA which is proposed by [18]. In dynFWA, the authors proved that Gaussian sparks could be removed from the algorithm without affecting its performance. Also, fireworks were separated into two different groups in dynFWA: 1) core fireworks (CF) 2) other fireworks. The CF's responsibility is to explore the vicinity of the local optimum location while other fireworks perform a global search. The amplitude of the explosions for each group is calculated individually. Algorithm 3 demonstrates the procedure of calculating the explosion amplitude for CF. The explosion amplitude of other fireworks is calculated from Eq. (12).

Algorithm 3. Dynamic explosion amplitude update for CF.

Algorithm
Initialization: Define:
$\mathrm{X_{CF}}$ (implies to the current location of the CF);
$\widehat{\mathrm{X}}_\mathrm{b}$ (implies to the best location among all explosion sparks);
$\mathrm{A_{CF}}$ (implies to the current explosion amplitude of the CF);
$\mathrm{C_a}$ (refers to the amplification coefficient);
$\mathrm{C_r}$ (refers to the reduction coefficient);
Iteration:
1: **if** $f\left(\widehat{\mathrm{X}}_\mathrm{b}\right) - f\left(\mathrm{X_{CF}}\right) < 0$ **then**
2: $\mathrm{A_{CF}} \leftarrow \mathrm{A_{CF}} * \mathrm{C_a}$;
3: **else**
4: $\mathrm{A_{CF}} \leftarrow \mathrm{A_{CF}} * \mathrm{C_r}$;
end if

The whole dynFWA framework is shown in the following algorithm:

Algorithm 4. dynFWA framework.

Algorithm
1: Initialization (of N fireworks and evaluation the quality)
2: Initialization (of the explosion amplitude for CF)
3: **while** termination criteria are not satisfied **do**
4: Calculation the number of explosion sparks
5: Calculation of the explosion amplitude for non-CF
6: **for** each firework **do**
7: Generation of explosion sparks
8: Mapping sparks at invalid locations back to search space
9: Evaluation of the quality of explosion sparks
10: **end for**
11: Updating the explosion amplitude of CF
12: Selecting the N fireworks for next iteration
13: **end while**

3.6. Modified fireworks algorithm

In this study, we used the FWA and changed its amplitude into a dynamic one. Also, two new operators were added to it to reduce its computational cost as well as enhancing its searching capabilities in marginal locations. In addition, after testing the MoFWA, it was observed that the existence of only one core firework is adequate for optimization. Also, we set the number of explosion sparks for each example, depending on the number of design variables and the size of search space to maintain the functionality of the algorithm. Moreover, the initial bounds of core firework were set so that the exploration capability of the algorithm be preserved.

3.6.1. Fly-back mechanism

Solutions to most mechanical problems are usually located in the vicinity of the feasible region's boundaries [29], [30]. Meanwhile, artificial algorithms face some challenges when they try to produce new solutions near those boundaries. In other words, when it comes to optimization close to the boundaries, some of the newly produced solutions may be located outside the feasible space. The fly-back mechanism ensures that all of the solutions are located within the feasible region by relocating the outer ones to their previous position [31]. Although flying back to the former location will guarantee an acceptable solution, it was observed that restoring half of the range between the initial location and the infeasible position is more effective than the previous method. This mechanism was implemented in the MoFWA to enhance its searching capabilities near the boundaries.

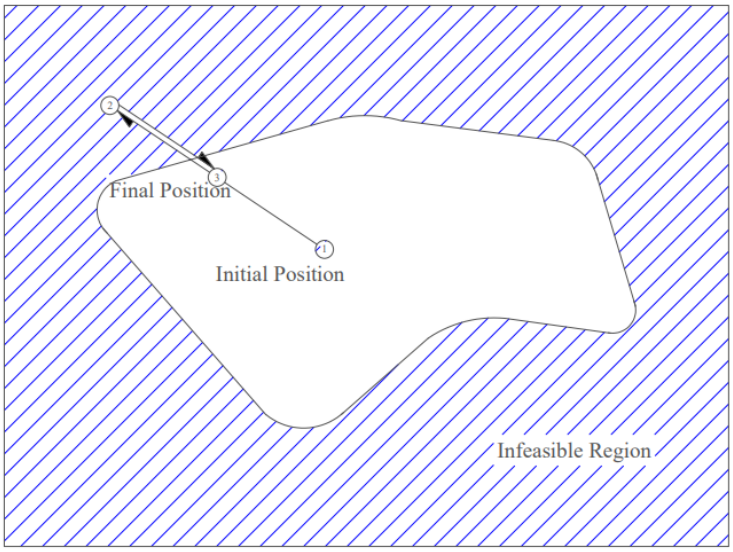

Fig. 1. Fly-back mechanism.

3.6.2. Duplicate sparks removal operator

When MoFWA reaches the global optima, its location could not get better much, so the explosion amplitude keeps multiplying to the reduction coefficient in every iteration. As a result, the explosion amplitude keeps shrinking. If the explosion amplitude is significantly reduced, it's possible that some of the sparks created may be the same as previous ones. This can result in increased computational cost and decreased speed for the MoFWA. To tackle this issue, we introduce the DSR operator that saves the sparks location of last two iterations to compare them with new sparks and to determine whether they are authentic or not. This procedure is explained in algorithm 5:

Algorithm 5. removing duplicate sparks.

Algorithm
1: survey s generated sparks
2: remove n-1 sparks from n similar sparks
3: compare s-(n-1) remaining sparks with last two generations
4: remove m similar sparks from current generation
5: evaluate remaining sparks
6: save the current and last generation for next iteration

3.6.3. Initial CF amplitude

In dynFWA, the initial CF amplitude was set manually. However, in MoFWA a new formula is introduced to calculate the initial CF amplitude automatically. After testing dynFWA numerous times under different circumstances, we concluded that the best size for the initial CF amplitude is around 60 percent of the total number of variables. The initial CF amplitude is calculated from Eq (13):

$$ICF\_amplitude = 0.6*\text{length(variables)} \quad (13)$$

Where ICF_amplitude is the initial core firework amplitude

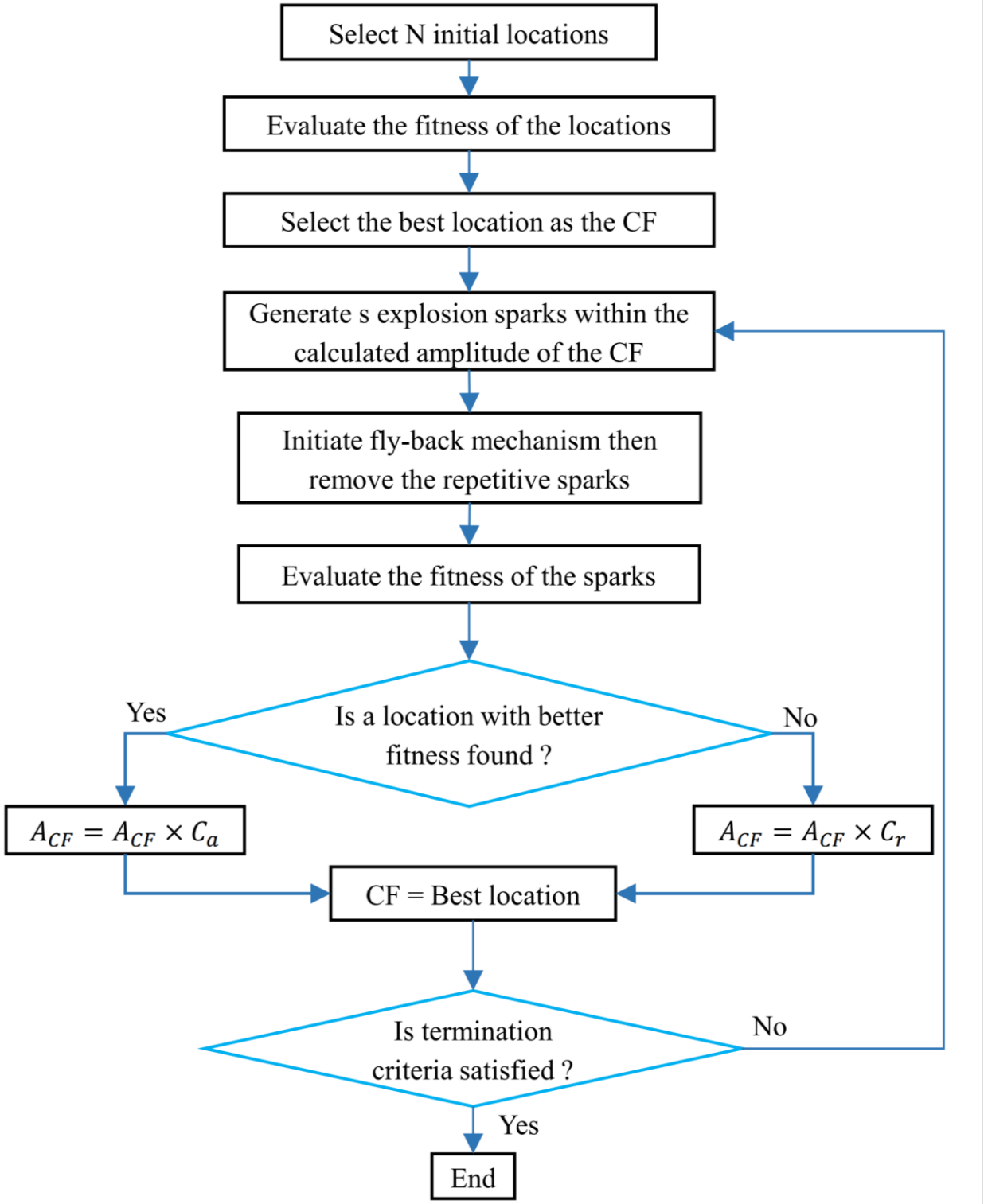
Select N initial locations
Evaluate the fitness of the locations
Select the best location as the CF
Generate s explosion sparks within the calculated amplitude of the CF
Initiate fly-back mechanism then remove the repetitive sparks
Evaluate the fitness of the sparks
Is a location with better fitness found ?
Yes
No
$A_{CF} = A_{CF} \times C_a$
$A_{CF} = A_{CF} \times C_r$
CF = Best location
Is termination criteria satisfied ?
No
Yes
End

Fig. 2. MoFWA algorithm flowchart.

4. Design examples

In this part, six steel structures including three trusses and three frames are presented to make a comparison between MoFWA and other algorithms. The design examples are:

- A 25-bar truss
- A 10-bar truss
- A 582-bar tower truss
- A two-bay three-story frame
- A one-bay 10-story frame
- A three-bay 24-story frame

The amplification (C_a) and reduction coefficient factors (C_r) were set to 1.2 and 0.9 for all of the examples. For each design example, 40 individual runs were carried out and the results of MoFWA were compared with FWA and also a wide range of other heuristic algorithms.

4.1. 25-bar space truss

The 25-bar transmission tower is frequently studied by numerous researchers with different methods. Fig. 3 shows topology and nodal numbering of the 25-bar space truss structure. The material density and modulus of elasticity were considered as 0.1 lb/in.^{3} (2767.99 kg/m^3) and 10,000 ksi (68,950 MPa), respectively. The loading condition is shown in Table 1. Maximum displacement for nodes 1 and 2 was limited to $\pm$0.35 in ($\pm$8.89 mm) in every direction, also the stress limit was considered as ±40 ksi (275.6MPa). Truss members were divided into 8 groups, Table 2 lists the grouping. The sections available for this problem were: {0.1, 0.2, 0.3, …, 2.5, 2.6, 2.8, 3.0, 3.2, 3.4} (in.^{2}). The sparks generation factor (M_e) was set to 150 for this example.

Table 1
Single load case for the 25-bar truss.

Node	Directions		
	x	y	Z
1	1.0	-10.0	-10.0
2	0	-10.0	-10.0
3	0.5	0	0
6	0.6	0	0

Table 2
Element information for the 25-bar truss.

Group	1	2	3	4	5	6	7	8
Elements	1	2-5	6-9	10,11	12,13	14-17	18-21	22-25

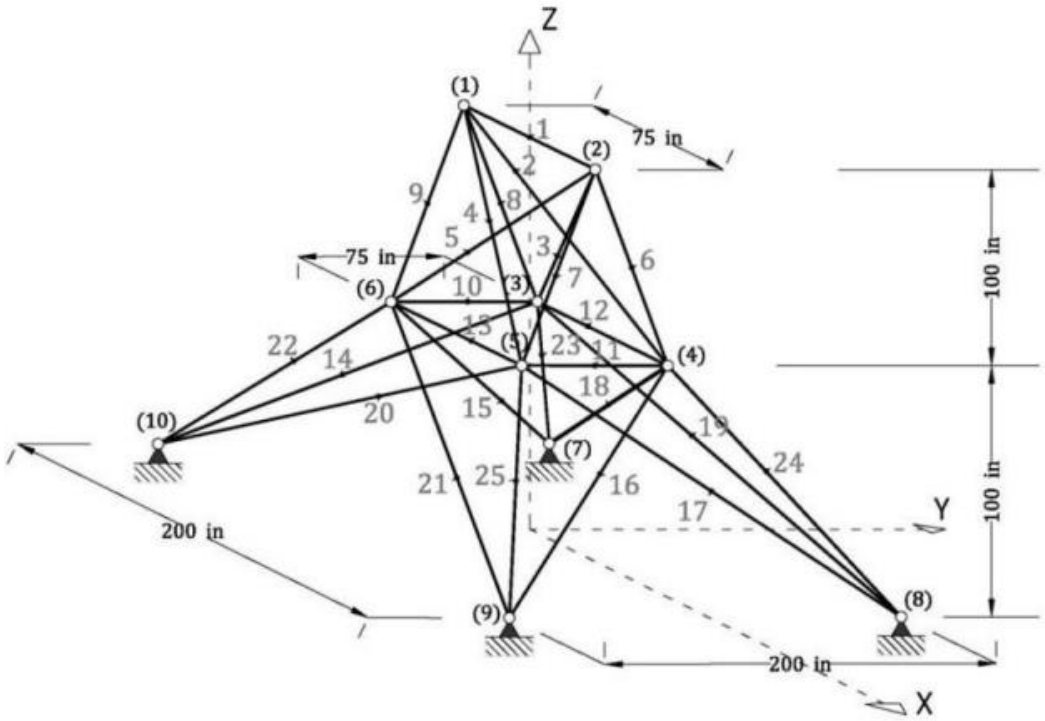

Fig. 3. Configuration of the first example.

Table 3
Optimal results of the 25-bar truss.

Design Variables		**Optimum cross section area ($in.^2$)**				
No	Des.Var.	MSCA [22]	NMA [23]	GWOM1 [24]	FWA	MoFWA
1	$A1$	0.1	0.1	0.1	0.1	0.1
2	$A2$~$A5$	0.3	0.3	0.6	0.4	0.4
3	$A6$~$A9$	3.4	3.4	3.4	3.4	3.4
4	$A10$~$A11$	0.1	0.1	0.1	0.1	0.1
5	$A12$~$A13$	2.1	2.1	2.3	1.8	1.8
6	$A14$~$A17$	1.0	1.0	1	0.9	0.9
7	$A18$~$A21$	0.5	0.5	0.2	0.6	0.6
8	$A22$~$A25$	3.4	3.4	3.4	3.4	3.4
Best (lb)		484.85	484.85	482.21	484.56	484.56
Average (lb)		484.94	484.94	N/A	498.39	488.73
Worst (lb)		N/A	N/A	N/A	546.24	495.03
Evaluation (#)		5000	250	N/A	8200	6000
Constraint violation		None	None	None	None	None

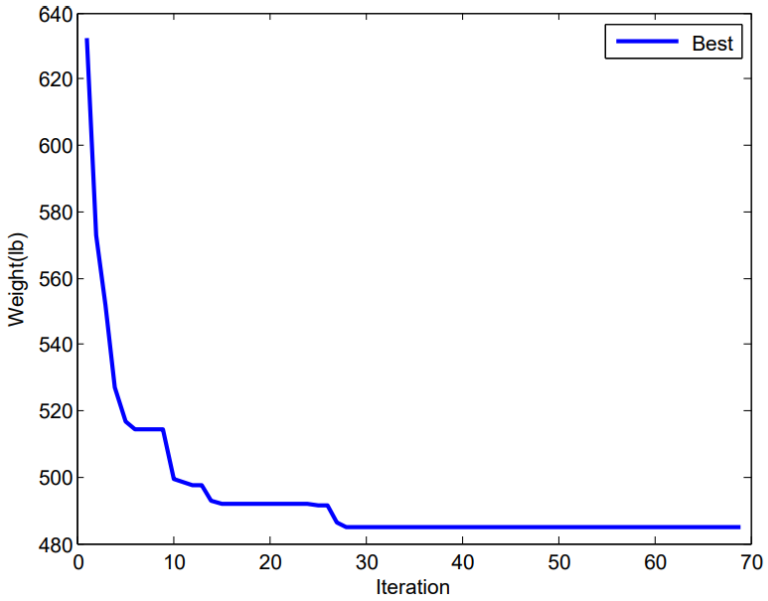

Fig. 4. Convergence history of 25-bar truss.

Table 3 lists the optimal designs of modified sine-cosine algorithm, newton meta-heuristic algorithm, improved grey wolf optimizer, FWA, and MoFWA. The FWA and MoFWA obtained the second-best weight of 484.56 lbs. The number of fitness function evaluations (FE) of MoFWA is 6000 which is less than FWA. Fig. 4 shows the convergence history of MoFWA for the twenty-five-bar truss reaching the optimal design in the 28th iteration.

4.2. Ten-bar planar truss

The second example is a 10-bar truss. The material density and modulus of elasticity are considered as 0.1 lb/in.^{3} (2767.99 kg/m^3) and 10,000 ksi (68,950 MPa), respectively. A single load $P_1 = 100$ kips is applied to nodes 4 and 2. The available cross-sectional areas for all members are mentioned in the following bracket:

A= {1.62, 1.80, 1.99, 2.13, 2.38, 2.62, 2.63, 2.88, 2.93, 3.09, 3.13, 3.38, 3.47, 3.55, 3.63, 3.84, 3.87, 3.88, 4.18, 4.22, 4.49, 4.59, 4.80, 4.97, 5.12, 5.74, 7.22, 7.97, 11.5, 13,5 13.9, 14.2, 15.5, 16.0, 16.9, 18.8, 1.99, 22.0, 22.9, 26.5, 30.0, 33.5} (in.^{2}).

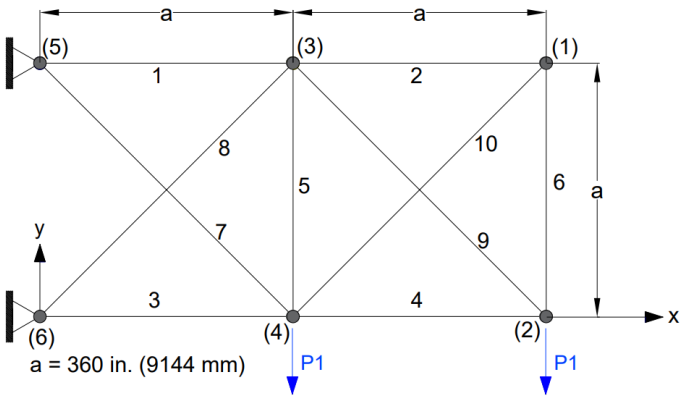

Fig. 5. Configuration of the 10-bar truss.

The allowable stress and nodal displacement are limited to ±25 ksi (±172.25 MPa) and ±2 in. (±50.8 mm). In this example, the sparks generation factor (M_e) is set to 150.

Table 4
Optimal results of the ten-bar truss.

Design Variables		**Optimum cross section area ($in.^2$)**				
No	Des.Var.	MSCA [22]	NMA [23]	GWOM1 [24]	FWA	MoFWA
1	$A1$	33.50	33.50	33.50	30.00	33.5
2	$A2$	1.62	1.62	1.62	1.62	1.62
3	$A3$	22.90	22.90	22.90	24.5	22
4	$A4$	14.20	14.20	14.20	15.5	15.5
5	$A5$	1.62	1.62	1.62	1.62	1.62
6	$A6$	1.62	1.62	1.62	1.62	1.62
7	$A7$	7.97	7.97	7.97	9.3	8.53
8	$A8$	22.90	22.9	22.9	22.0	22.0
9	$A9$	22.00	22.0	22.0	22.0	22.0
10	$A10$	1.62	1.62	1.62	1.62	1.62
Best (lb)		5,490.74	5,490.74	5,490.74	5,490.74	5476.32
Average (lb)		5492.64	5,490.91	N/A	5,502.4	5493.615
Worst (lb)		N/A	N/A	N/A	5,534.7	5525.026
Evaluation (#)		10000	2880	N/A	18,000	6560
Constraint violation		None	None	None	None	None

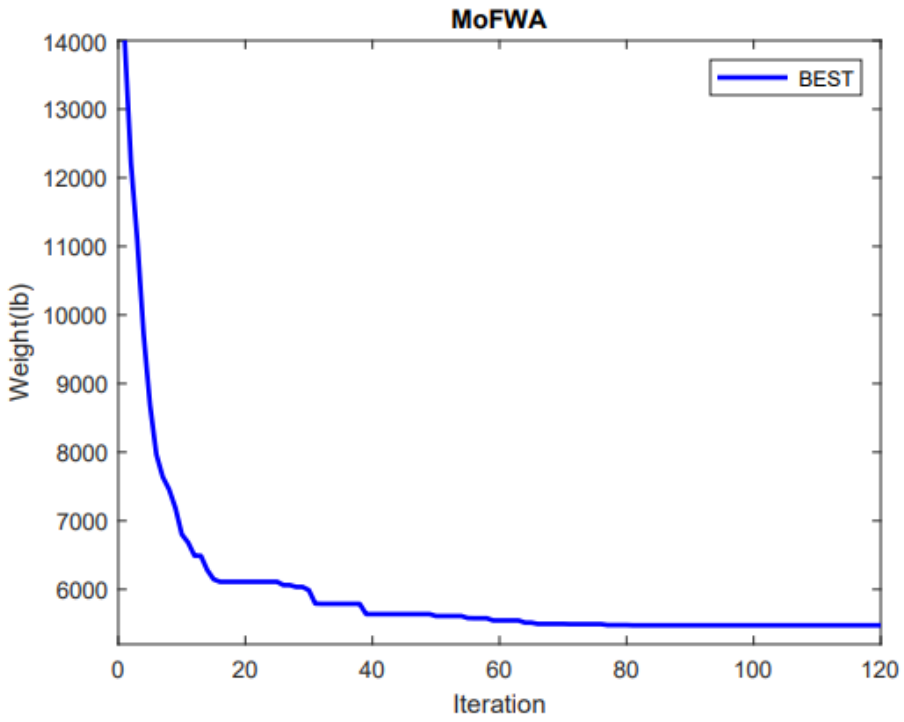

Fig. 6. Convergence history of 10-bar truss.

Table 4 lists the optimal design of mentioned algorithms. In this example, MoFWA obtained the best weight of 5476.32 lbs with a total evaluation of 6560, which outranks FWA and other algorithms. Fig. 6 demonstrates the convergence history of MoFWA for the ten-bar truss example. All in all, it is obvious that MoFWA has the best performance among all of the mentioned algorithms.

4.3. 582-bar tower truss

The last truss structure in this study is a 582-bar tower truss which can be seen in Fig. 7. The material density and modulus of elasticity were considered as 0.283 lb/in.^{3} (7,833.4 kg/m^3) and 29,000 ksi (200 GPa), respectively. The members of this truss were divided into 32 groups of design variables. A single load case was considered consisting of lateral loads of 5.0 KN (1.12 kips) applied in both x and y directions and a vertical load of 30 KN (6.74 kips) applied in the z-direction to all nodes of the tower. According to Table 5, a set of 140 standard steel sections are considered for this problem. The maximum nodal displacement is limited to $\pm$8.0 cm (3.15 in.) in every direction, and stress limitations are defined as provisions of ASD-AISC. In this example, the sparks generation factor (M_e) is set to 200.

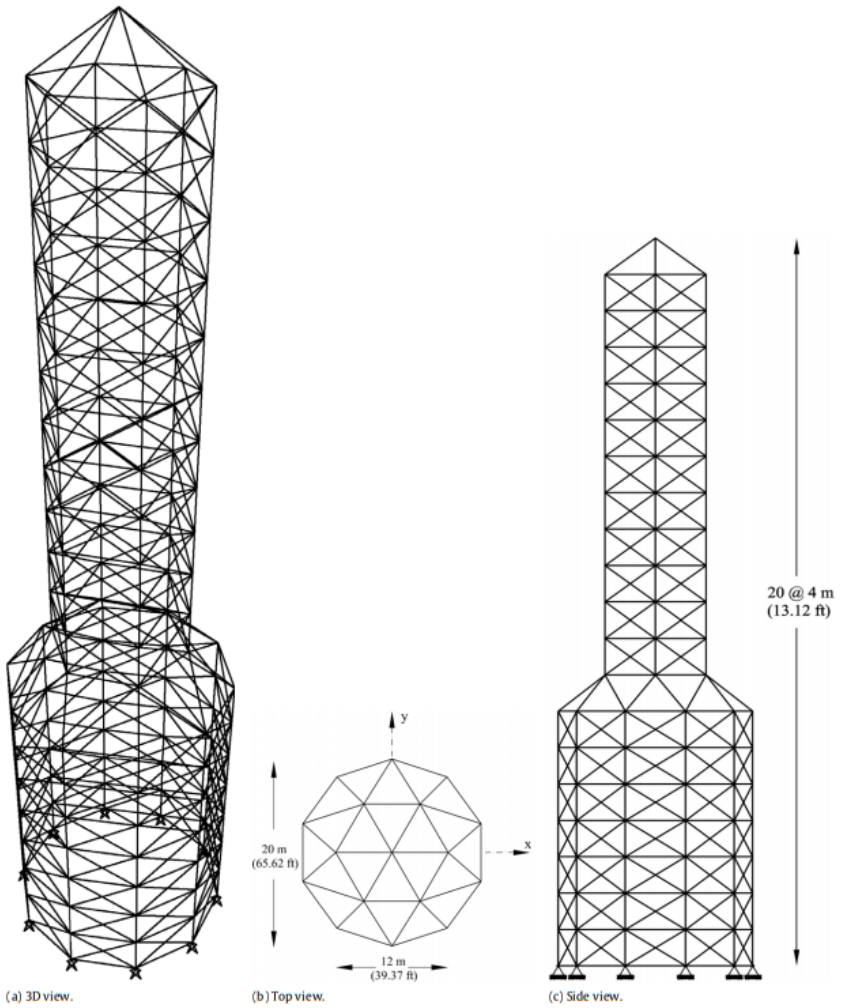

Fig. 7. Configuration of the 582-bar tower truss.

Table 5
Profile list from AISC code for the 582-bar tower truss.

No.	section	cm^2	No.	section	cm^2	No.	section	cm^2
1	W8X21	39.74	48	W12X58	109.68	95	W21X111	210.97
2	W12X22	41.81	49	W8X58	110.32	96	W10X112	212.26
3	W14X22	41.87	50	W18X60	113.55	97	W27X114	216.13
4	W10X22	41.87	51	W10X60	113.55	98	W24X117	221.94
5	W8X24	45.68	52	W14X61	115.48	99	W18X119	226.45
6	W10X26	49.10	53	W24X62	118.06	100	W14X120	227.74
7	W12X26	49.35	54	W21X62	118.06	101	W12X120	227.74
8	W16X26	49.55	55	W18X65	123.23	102	W21X122	231.61
9	W14X26	49.61	56	W12X65	123.23	103	W24X131	248.39
10	W8X28	53.16	57	W8X67	127.10	104	W21X132	250.32
11	W12X30	56.71	58	W21X68	129.03	105	W14X132	250.32
12	W10X30	57.03	59	W16X67	129.03	106	W12X136	257.42
13	W14X30	57.10	60	W14X68	129.03	107	W14X145	275.48
14	W8X31	58.84	61	W10X68	129.03	108	W24X146	277.42
15	W16X31	58.90	62	W24X68	129.68	109	W27X146	278.06
16	W10X33	62.65	63	W18X71	134.19	110	W21X147	278.71
17	W14X34	64.52	64	W12X72	136.13	111	W12X152	288.39
18	W18X35	66.45	65	W21X73	138.71	112	W14X159	301.29
19	W12X35	66.45	66	W14X74	140.64	113	W27X161	307.10
20	W8X35	66.45	67	W18X76	143.87	114	W24X162	307.74
21	W16X36	68.39	68	W24X76	144.52	115	W12X170	322.58
22	W14X38	72.26	69	W10X77	145.81	116	W14X176	334.19
23	W10X39	74.19	70	W16X77	147.74	117	W27X178	338.71
24	W12X40	75.48	71	W12X79	149.68	118	W12X190	360.00
25	W8X40	75.48	72	W14X82	154.84	119	W14X193	366.45
26	W18X40	76.13	73	W21X83	156.77	120	W12X210	398.71
27	W16X40	76.13	74	W24X84	159.35	121	W14X211	400.00
28	W14X43	81.29	75	W27X84	160.00	122	W12X230	436.77
29	W21X44	83.87	76	W18X86	163.23	123	W14X233	441.93
30	W12X45	84.52	77	W12X87	165.16	124	W12X252	477.42
31	W16X45	85.81	78	W10X88	167.10	125	W14X257	487.74
32	W10X45	85.81	79	W16X89	170.32	126	W12X279	528.39
33	W18X46	87.10	80	W14X90	170.97	127	W14X283	537.42
34	W14X48	90.97	81	W21X93	176.13	128	W12X305	578.06
35	W8X48	90.97	82	W27X94	178.71	129	W14X311	589.68
36	W10X49	92.90	83	W24X94	178.71	130	W12X336	637.42
37	W12X50	94.19	84	W12X96	181.94	131	W14X342	651.61
38	W21X50	94.84	85	W18X97	183.87	132	W14X370	703.22
39	W18X50	94.84	86	W14X99	187.74	133	W14X398	754.84
40	W16X50	94.84	87	W10X100	189.68	134	W14X426	806.45
41	W14X53	100.64	88	W16X100	191.61	135	W14X455	864.51
42	W12X53	100.64	89	W21X101	192.26	136	W14X500	948.39
43	W10X54	101.94	90	W27X102	193.55	137	W14X550	1045.16
44	W18X55	104.52	91	W24X104	197.42	138	W14X605	1148.38
45	W24X55	105.16	92	W18X106	200.64	139	W14X665	1264.51
46	W21X57	107.74	93	W12X106	201.29	140	W14X730	1387.09
47	W16X57	108.39	94	W14X109	206.45			

Table 6
Optimization results of the 582-bar truss.

variables	Optimal W-shaped sections				
No	STA [25]	ABC [15]	CBO [26]	FWA	MoFWA
1	W8x21	W8x21	W8x21	W8x24	W8x21
2	W10x68	W18x86	W12x79	W24x84	W24x84
3	W8x21	W8x24	W8x28	W8x28	W8x21
4	W10x77	W10x60	W10x60	W18x71	W18x71
5	W8x21	W8x24	W8x24	W8x24	W8x21
6	W8x21	W8x21	W8x21	W8x24	W8x21
7	W10x60	W10x49	W10x68	W10x49	W10x60
8	W8x21	W8x24	W8x24	W8x24	W8x21
9	W8x21	W8x21	W8x21	W8x24	W8x21
10	W14x48	W12x53	W14x48	W14x48	W14x48
11	W8x21	W8x24	W12x26	W12x30	W8x21
12	W14x74	W21x62	W21x62	W24x76	W24x76
13	W16x67	W27x84	W18x76	W27x84	W18x76
14	W12x65	W10x45	W12x53	W10x49	W14x48
15	W12x65	W27x84	W14x61	W27x84	W10x100
16	W8x21	W8x31	W8x40	W8x31	W8x21
17	W12x65	W8x21	W10x54	W14x61	W14x34
18	W8x21	W12x53	W12x26	W12x53	W12x40
19	W8x21	W8x24	W8x21	W8x21	W8x21
20	W10x68	W10x22	W14x43	W12x40	W14x34
21	W8x21	W16×36	W8x24	W16x36	W14x38
22	W8x21	W8×24	W8x21	W8x24	W8x21
23	W10x22	W8x21	W10x22	W8x31	W14x22
24	W8x21	W10×22	W8x24	W8x28	W12x26
25	W12x40	W6×25	W8x21	W8x21	W8x21
26	W6x25	W8x21	W8x21	W8x21	W8x21
27	W10x22	W8x21	W8x24	W8x24	W8x21
28	W8x21	W8x24	W8x21	W8x28	W8x21
29	W8x28	W8x21	W8x21	W16x36	W12x22
30	W10x22	W10x22	W6x25	W8x24	W8x21
31	W16x36	W8x24	W10x33	W8x24	W8x21
32	W12x53	W6x25	W8x28	W8x24	W8x21
Weight (lb)	364,143.43	368,484.1	376,344.74	401,895.6	360,456.22
Evaluation (#)	6000	50000	6400	58,000	41,000
1 lb = 0.45359 Kg					

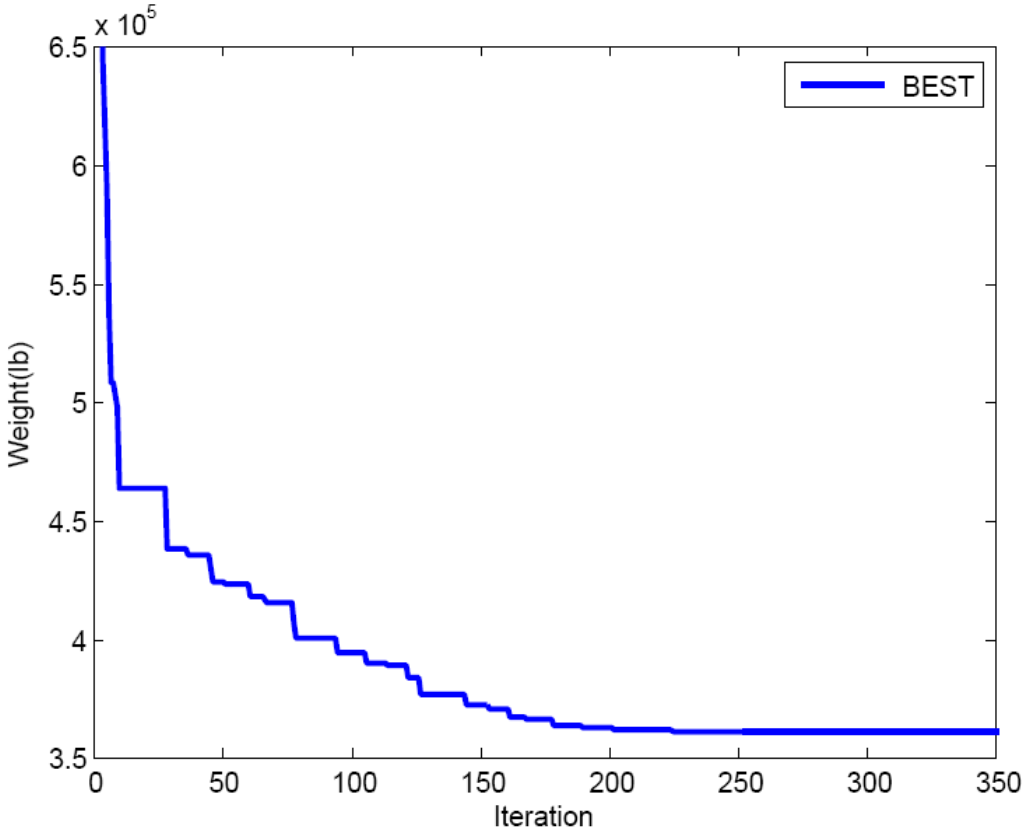

Fig. 8. convergence history of 582-bar truss.

Table 6 illustrates the optimum W-shaped sections and minimum weights that are derived from MoFWA and other algorithms. MoFWA's design weighs 360,456.22 lbs which is the best among all of the algorithm's results. Fig. 8 demonstrates the convergence curve of MoFWA algorithm for the 582-bar truss.

4.4. 2-bay, three-story frame

In Fig. 9, the topology and loading conditions of a 2-bay three-story frame are depicted. This frame consists of 15 members, which can be categorized into two groups. We have chosen 267 standard W-shape profiles for the beams and limited the columns to W10 sections. Table 7 lists all of the available profiles. This frame is optimized according to the AISC-LRFD specifications. Also, displacement constraints are not considered. In this example, the modulus of elasticity of steel is taken as E = 200 GPa (29,000 ksi), the yield stress is considered as Fy = 248.2 MPa (36 ksi) and the material unit weight of γ = 7861 kg/m^3 (0.284 lb/in.^{3}) is used. Each column is considered unbraced along its length, and the unbraced length of each beam member is specified as one-sixth of span length. In this example, the sparks generation factor (M_e) is set to 50.

Table 7
Profile list from ASIC code (2009).

W-shape profile list							
W6X8.5	W8X31	W21X57	W16X89	W21X132	W12X190	W27X258	W36X359
W6X9	W16X31	W16X57	W14X90	W14X132	W30X191	W36X260	W30X357
W8X10	W10X33	W12X58	W21X93	W30X132	W24X192	W30X261	W40X362
W10X12	W14X34	W8X58	W27X94	W36X135	W14X193	W44X262	W27X368
W6X12	W18X35	W18X60	W24X94	W12X136	W36X194	W33X263	W40X372
W4X13	W12X35	W10X60	W12X96	W33X141	W27X194	W40X264	W24X370
W8X13	W8X35	W14X61	W18X97	W18X143	W40X199	W40X277	W14X370
W12X14	W16X36	W24X62	W30X99	W14X145	W33X201	W40X278	W33X387
W10X15	W14X38	W21X62	W14X99	W24X146	W21X201	W12X279	W40X392
W8X15	W10X39	W18X65	W10X100	W27X146	W24X207	W24X279	W30X391
W6X15	W12X40	W12X65	W16X100	W21X147	W36X210	W36X280	W36X393
W12X16	W8X40	W8X67	W21X101	W30X148	W12X210	W27X281	W40X397
W5X16	W18X40	W16X67	W27X102	W40X149	W40X211	W14X283	W14X398
W6X16	W16X40	W21X68	W24X103	W36X150	W14X211	W33X291	W14X426
W10X17	W14X43	W14X68	W24X104	W12X152	W30X211	W44X290	W40X431
W8X18	W21X44	W10X68	W18X106	W33X152	W40X215	W30X292	W36X439
W5X19	W12X45	W24X68	W12X106	W18X158	W27X217	W40X297	W14X455
W12X19	W16X45	W18X71	W30X108	W14X159	W33X221	W36X300	W14X500
W10X19	W10X45	W12X72	W14X109	W36X160	W24X229	W12X305	W40X503
W6X20	W18X46	W21X73	W21X111	W27X161	W36X230	W24X306	W36X527
W8X21	W21X48	W14X74	W10X112	W24X162	W44X230	W27X307	W27X539
W12X22	W14X48	W18X76	W27X114	W21X166	W12X230	W14X311	W14X550
W14X22	W8X48	W24X76	W30X116	W40X167	W36X232	W33X318	W40X593
W10X22	W10X49	W10X77	W24X117	W33X169	W14X233	W40X324	W14X605
W8X24	W12X50	W16X77	W33X118	W12X170	W40X235	W30X326	W36X650
W6X25	W21X50	W12X79	W18X119	W36X170	W30X235	W40X327	W14X665
W10X26	W18X50	W14X82	W14X120	W30X173	W27X235	W36X328	W14X730
W12X26	W16X50	W21X83	W12X120	W18X175	W33X241	W40X331	W36X798
W16X26	W14X53	W24X84	W21X122	W24X176	W36X245	W44X335	W14X808
W14X26	W12X53	W27X84	W30X124	W14X176	W40X249	W24X335	
W8X28	W10X54	W18X86	W27X129	W27X178	W24X250	W12X336	
W12X30	W21X55	W12X87	W18X130	W36X182	W12X252	W27X336	
W10X30	W18X55	W10X88	W33X130	W21X182	W36X256	W14X342	
W14X30	W24X55	W30X90	W24X131	W40X183	W14X257	W33X354	

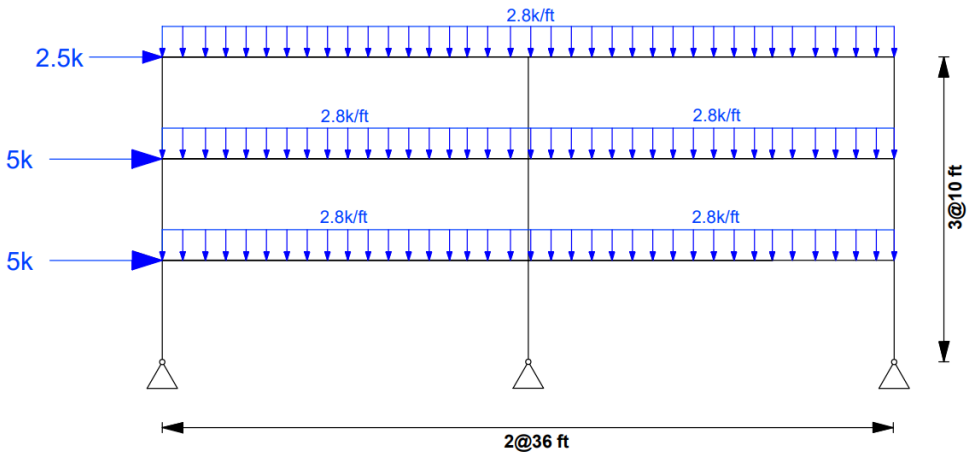

Fig. 9. Fig Configuration of the two-bay, three-story frame.

Table 8
Optimization results of the two-bay, three-story frame.

Variables		Optimal W-shaped sections				
No	Des.Var.	*MHBMO* [27]	IHS [28]	DDHS [13]	FWA	MoFWA
1	beams	W24x62	W24x62	W24x62	W14x61	W14x61
2	*columns*	W10x49	W10x60	W10x60	W10x49	W10x49
Weight (lb)		17,789	18,792	18,792	17,549.55	17,549.55
Evaluation (#)		650	N/A	270	480	270

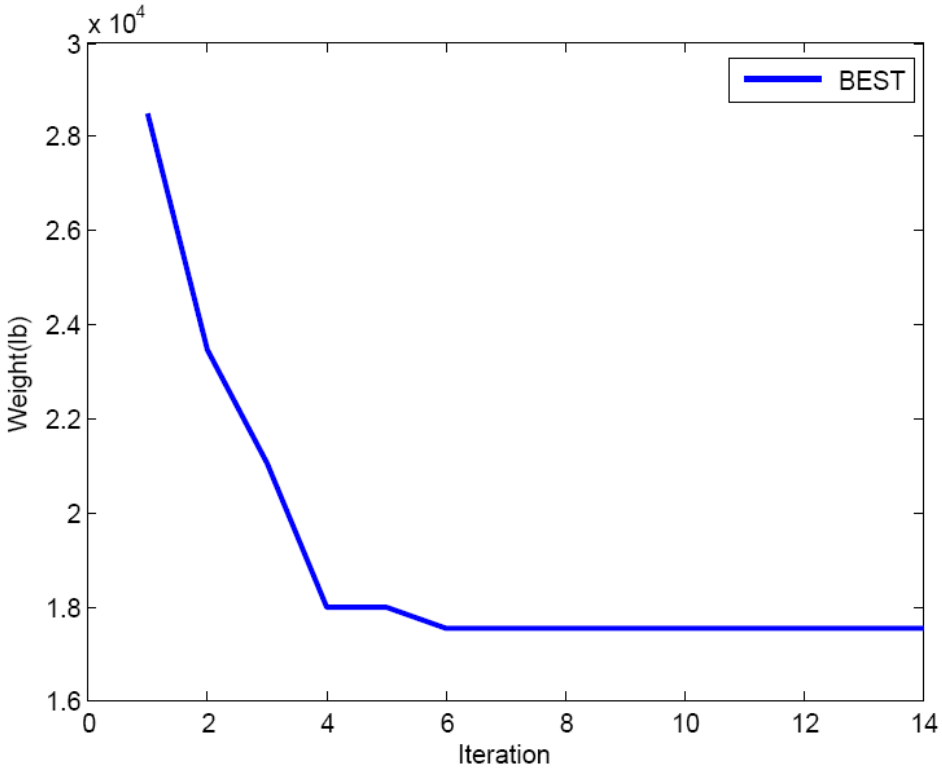

Fig. 10. Convergence history of two-bay, three-story frame.

Table 8 lists the best designs developed by MoFWA, and other algorithms. MoFWA designed a frame weighing 17,549.55 lbs which is lighter than the designs of other algorithms. Fig. 10 shows the convergence curve of MoFWA reaching the optimal weight in the 6th iteration.

4.5. one-bay, ten-story frame

Fig. 11 demonstrates the topology and loading condition of the one-bay ten-story frame. This structure has 30 members that are grouped into 9 groups. The beams are chosen from Table7 while column selection is limited to W12 and W14 sections. The frame is designed following the AISC-LRFD specifications with a maximum inter-story drift constraint of story-height/300. In addition, Young's modulus is considered as E=29,000 ksi, and yield stress is considered as fy = 36 ksi. In this example, the sparks generation factor (M_e) is set to 50.

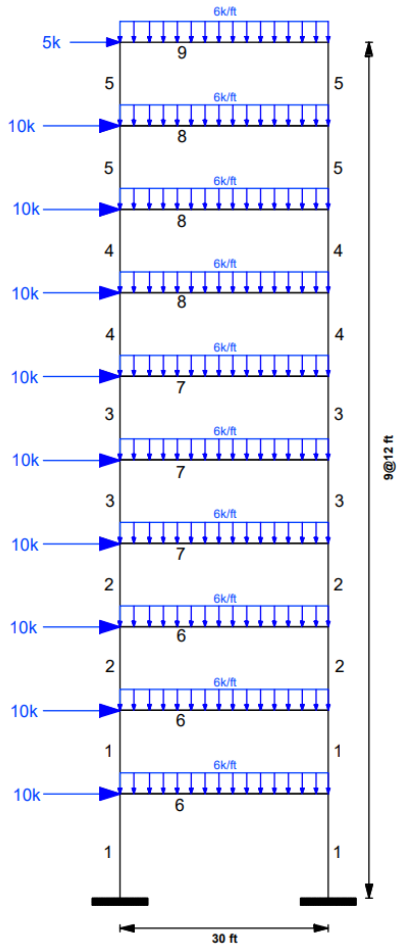

Fig. 11. topology of the 0ne-bay, ten-story frame.

Table 9
Optimization results of one-bay, ten-story frame.

Variables		Optimal W-shaped sections				
No	Des.Var.	SBO [29]	MHBMO [27]	CS [11]	FWA	MoFWA
1	A_1~A_4	W14x233	W14x233	W14x233	W14x233	W14x233
2	A_5~A_8	W14x176	W14x176	W14x176	W14x176	W14x176
3	A_9~A_{12}	W14x145	W14x145	W14x132	W14x145	W14x132
4	A_{13}~A_{16}	W14x99	W14x99	W14x109	W14x99	W14x109
5	A_{17}~A_{20}	W14x61	W14x61	W14x61	W12x65	W12x61
6	A_{21}~A_{23}	W30x108	W30x108	W33x118	W33x118	W33x118
7	A_{24}~A_{26}	W30x90	W30x90	W30x108	W30x99	W30x108
8	A_{27}~A_{29}	W27x84	W27x84	W24x55	W27x84	W24x55
9	A_{30}	W18x46	W21x44	W18x40	W14x53	W18x40
Best (lb)		62,430	61,617	62,074	64,408.2	62,074
Evaluation (#)		11,677	3600	4438	3200	1600

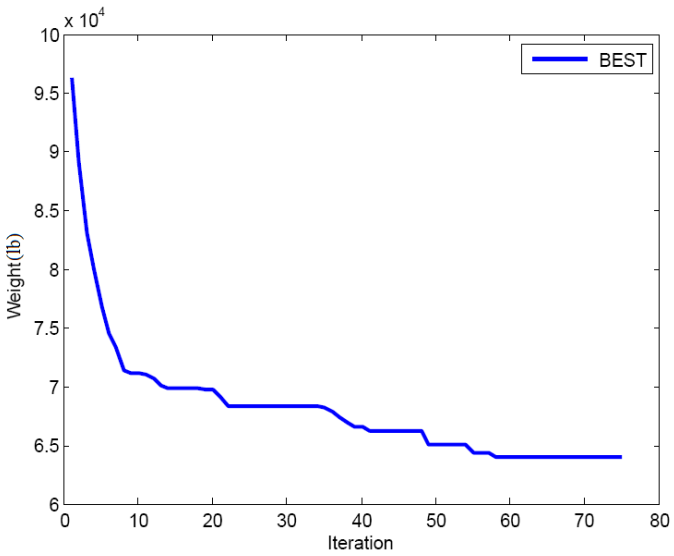

Fig. 12. Convergence history of one-bay, ten-story frame.

Table 9 shows the results of different algorithms optimizing the one-bay ten-story frame. The convergence history can be seen in Fig. 12. MoFWA obtained the optimal weight of 62,074 lbs which is second-best among other algorithms. However, MoFWA has fewer evaluations than other algorithms.

Table 10
Optimization results of three-bay, 24-story frame.

Variables	**Optimal W-shaped sections**					
No	TLBO [30]	MHBMO [27]	SBO [29]	EWOA [31]	FWA	MoFWA
1	W30x90	W30×90	W30x90	W30x90	W30x90	W30x90
2	W8x18	W8×18	W8x18	W10x30	W6x20	W5x16
3	W24x62	W24×55	W21x48	W24x55	W21x44	W21x44
4	W6x9	W14×22	W6x8.5	W6x8.5	W6x9	W6x8.5
5	W14x132	W14×145	W14x152	W14x159	W14x159	W14x159
6	W14x120	W14×120	W14x120	W14x99	W14x145	W14x145
7	W14x99	W14×99	W14x109	W14x120	W14x132	W14x132
8	W14x82	W14×82	W14x74	W14x74	W14x99	W14x99
9	W14x74	W14×68	W14x82	W14x74	W14x68	W14x68
10	W14x53	W14×53	W14x43	W14x43	W14x61	W14x53
11	W14x34	W14×30	W14x34	W14x30	W14x43	W14x34
12	W14x22	W14×22	W12x19	W14x22	W14x22	W14x22
13	W14x109	W14×120	W14x109	W14x90	W14x109	W14x109
14	W14x99	W14×109	W14x109	W14x120	W14x109	W14x99
15	W14x99	W14×99	W14x99	W14x90	W14x90	W14x90
16	W14x90	W14×90	W14x99	W14x99	W14x82	W14x82
17	W14x68	W14×68	W14x68	W14x68	W14x74	W14x68
18	W14x53	W14×53	W14x61	W14x61	W14x43	W14x48
19	W14x34	W14×30	W14x34	W14x43	W14x30	W14x30
20	W14x22	W14×22	W14x22	W14x22	W14x26	W14x22
Weight (KN)	903.54	901.895	900.42	905.17	912.26	900.24
Evaluation (#)	12,000	6000	14,572	18,820	37,500	25,000
1 KN = 224.81 lb						

4.6. three-bay, twenty-four-story frame

The last design example is a three-bay twenty-four-story frame which is shown in Fig. 13 consisting of 168 members that are divided into 20 group. The yield stress and modulus of elasticity are considered as 230.3 MPa and 205 GPa, respectively. All beams are chosen from 267 W-shape sections from Table 7 and all of the columns are restricted to W14 sections. This frame is optimized according to the AISC-LRFD specifications with inter-story drift constraints of H/300. In this example, the sparks generation factor (M_e) is set to 250.

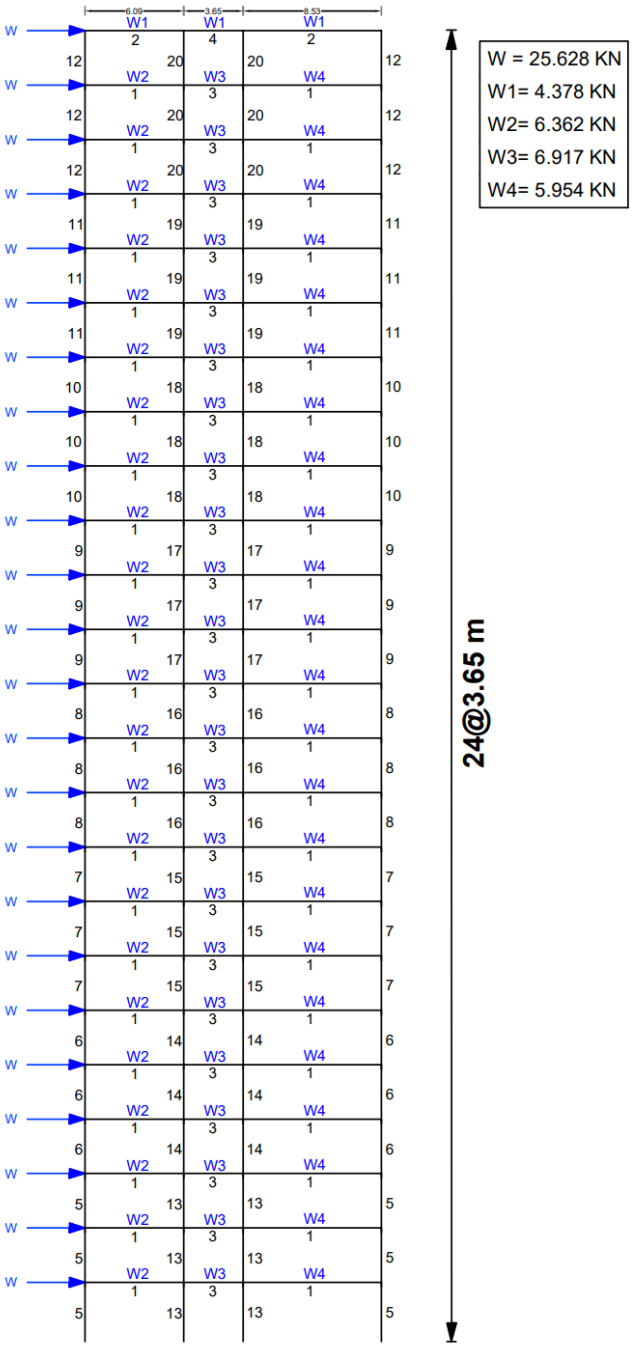

Fig. 13. Configuration of the three-bay, 24-story frame.

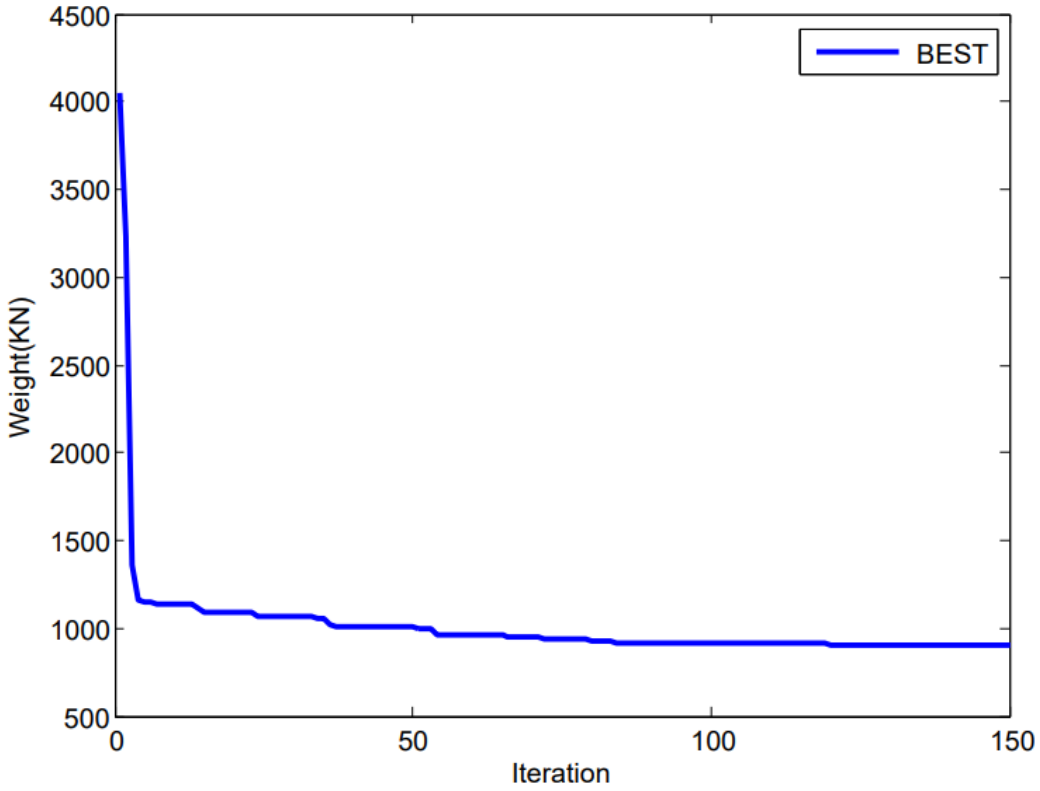

Fig. 14. Convergence history of three-bay, 24-story frame.

Table 10 indicates that the MoFWA algorithm achieved the best weight of 900.24 KN for 3-bay, 24-story frame. However, it took more evaluations for MoFWA to find the best result. Fig. 14 illustrates the convergence history of MoFWA.

5. Conclusions

In this article, a modified version of the fireworks algorithm called MoFWA was introduced. FWA had some deficiencies causing the algorithm to have higher computational cost. To tackle this issue, some strategies were implemented into FWA to enhance its performance in finding the global optimum and reducing its computational cost. The modifications made on FWA are: 1) adding the fly-back mechanism 2) introducing the duplicate sparks removal operator, and 3) Using a dynamic amplitude and setting a new formula for the calculation of the initial amplitude.

The dynamic amplitude, the initial CF amplitude, the reduction coefficient, the amplification coefficient, the sparks generation factor, the duplicate sparks removal operator, and the number of fireworks are the main controlling parameters of MoFWA and the accuracy of designs along with computational efficiency of the algorithm depend on them.

In order to compare MoFWA with the original FWA and other metaheuristics, they were tested on six steel structures. As mentioned before, the objective function of these problems was to minimize the total weight of the structures and constraints were beam/column design strength and maximum allowable inter-story drift specified in AISC-LRFD.

In five out of six examples, MoFWA performed brilliantly and attained lighter structures with less computational cost than other algorithms, especially FWA. The results show the vast applicability of the MoFWA algorithm. MoFWA produced comparably accurate and robustness results, with low computational cost for both large and small structures. In addition, MoFWA outperformed FWA in all of the examples, achieving better results with lower computational cost. However, Overcoming the difficulty of getting stuck in a local minimum, like many other algorithms, remains a challenge for MoFWA. It may be beneficial to introduce an appropriate mutation operator in future studies.

To sum up, the changes made to MoFWA have proven to be highly beneficial, surpassing the performance of the initial FWA, particularly in terms of function evaluations. Furthermore, the inclusion of the fly-back mechanism has enhanced its ability to exploit marginal regions effectively.

References

[1] Kripka M. Discrete optimization of trusses by simulated annealing. J Brazilian Soc Mech Sci Eng 2004;26:170–3. https://doi.org/10.1590/S1678-58782004000200008.

[2] Camp C V., Farshchin M. Design of space trusses using modified teaching-learning based optimization. Eng Struct 2014;62–63:87–97. https://doi.org/10.1016/j.engstruct.2014.01.020.

[3] Dede T, Ayvaz Y. Structural optimization with teaching-learning-based optimization algorithm. Struct Eng Mech 2013;47. https://doi.org/10.12989/sem.2013.47.4.495.

[4] Babaei M, Sanaei E. Multi-objective optimal design of braced frames using hybrid genetic and ant colony optimization. Front Struct Civ Eng 2016;10:472–80. https://doi.org/10.1007/s11709-016-0368-4.

[5] Babaei M, Mollayi M. Multi-objective Optimization of Reinforced Concrete Frames Using NSGA-II Algorithm. Eng Struct Technol 2016;8:157–64. https://doi.org/10.3846/2029882X.2016.1250230.

[6] Babaei M, Taghaddosi N, Seraji N. Optimal Design of MR Dampers Using NSGA-II Algorithm. J Soft Comput Civ Eng 2023;7:72–92. https://doi.org/10.22115/scce.2022.347247.1466.

[7] Hasançebi O, Çarbaş S, Doğan E, Erdal F, Saka MP. Performance evaluation of metaheuristic search techniques in the optimum design of real size pin jointed structures. Comput Struct 2009;87:284–302. https://doi.org/10.1016/j.compstruc.2009.01.002.

[8] Varaee H, Safaeian Hamzehkolaei N, Safari M. A Hybrid Generalized Reduced Gradient-Based Particle Swarm Optimizer for Constrained Engineering Optimization Problems. J Soft Comput Civ Eng 2021;5:86–119. https://doi.org/10.22115/scce.2021.282360.1304.

[9] Mashayekhi MR, Shirpour A, Sadeghi R. Finding Optimum Parameters of Passive Tuned Mass Damper by PSO, WOA, and Hybrid PSO-WOA (HPW) Algorithms. J Soft Comput Civ Eng 2023;7:72–92. https://doi.org/10.22115/scce.2023.352340.1489.

[10] Sanaei E, Babaei M. Cellular Automata in Topology Optimization of Continuum Structures. Int J Eng Sci Technol 2011;3. https://doi.org/10.4314/ijest.v3i4.68538.

[11] Kaveh A, Bakhshpoori T. Optimum design of steel frames using Cuckoo Search algorithm with Lévy flights. Struct Des Tall Spec Build 2013;22:1023–36. https://doi.org/10.1002/tal.754.

[12] Kaveh A, Ahmadi B. Sizing, geometry and topology optimization of trusses using force method and supervised charged system search. Struct Eng Mech 2014;50:365–82. https://doi.org/10.12989/sem.2014.50.3.365.

[13] Murren P, Khandelwal K. Design-driven harmony search (DDHS) in steel frame optimization. Eng Struct 2014;59:798–808. https://doi.org/10.1016/j.engstruct.2013.12.003.

[14] Sadollah A, Eskandar H, Bahreininejad A, Kim JH. Water cycle, mine blast and improved mine blast algorithms for discrete sizing optimization of truss structures. Comput Struct 2015;149:1–16. https://doi.org/10.1016/j.compstruc.2014.12.003.

[15] Sonmez M. Discrete optimum design of truss structures using artificial bee colony algorithm. Struct Multidiscip Optim 2011;43:85–97. https://doi.org/10.1007/s00158-010-0551-5.

[16] Babaei M, Mollayi M. An improved constrained differential evolution for optimal design of steel frames with discrete variables. Mech Based Des Struct Mach 2020;48:697–723. https://doi.org/10.1080/15397734.2019.1657890.

[17] Tan Y, Zhu Y. Fireworks algorithm for optimization. Lect Notes Comput Sci (Including Subser Lect Notes Artif Intell Lect Notes Bioinformatics) 2010;6145 LNCS:355–64. https://doi.org/10.1007/978-3-642-13495-1_44.

[18] Zheng S, Janecek A, Li J, Tan Y. Dynamic search in fireworks algorithm. Proc 2014 IEEE Congr Evol Comput CEC 2014 2014:3222–9. https://doi.org/10.1109/CEC.2014.6900485.

[19] Gholizadeh S, Milany A. An improved fireworks algorithm for discrete sizing optimization of steel skeletal structures. Eng Optim 2018;50:1829–49. https://doi.org/10.1080/0305215X.2017.1417402.

[20] Barraza J, Melin P, Valdez F, Gonzalez CI. Fuzzy FWA with dynamic adaptation of parameters. 2016 IEEE Congr Evol Comput CEC 2016 2016:4053–60. https://doi.org/10.1109/CEC.2016.7744304.

[21] Sanaei E, Babaei M. Topology optimization of structures using cellular automata with constant strain triangles. Int J Civ Eng 2012;10:179–88.

[22] Gholizadeh S, Sojoudizadeh R. Modified sine-cosine algorithm for sizing optimization of truss structures with discrete design variables. Iran Univ Sci Technol 2019;9:195–212.

[23] Danesh M, Jalilkhani M. Sizing optimization of truss structures with newton meta-heuristic algorithm. Int J Optim Civ Eng 2020;10:433–50.

[24] Alkhraisat H, Dalbah LM, Al-Betar MA, Awadallah MA, Assaleh K, Deriche M. Size Optimization of Truss Structures Using Improved Grey Wolf Optimizer. IEEE Access 2023;11:13383–97. https://doi.org/10.1109/ACCESS.2023.3243164.

[25] Shahrouzi M. Switching teams algorithm for sizing optimization of truss structures. Int J Optim Civ Eng 2020;10:365–89.

[26] Kaveh A, Mahdavi VR. Colliding Bodies Optimization method for optimum discrete design of truss structures. Comput Struct 2014;139:43–53. https://doi.org/10.1016/j.compstruc.2014.04.006.

[27] Afzali SH, Darabi A, Niazkar M. Steel frame optimal design using MHBMO algorithm. Int J Steel Struct 2016;16:455–65. https://doi.org/10.1007/s13296-016-6016-y.

[28] Mosharmovahhed M, Moharrami H. Design optimization of moment frame structures by the method of inscribed hyperspheres. Struct Multidiscip Optim 2021;64:335–48. https://doi.org/10.1007/s00158-021-02869-4.

[29] Farshchin M, Maniat M, Camp C V., Pezeshk S. School based optimization algorithm for design of steel frames. Eng Struct 2018;171:326–35. https://doi.org/10.1016/j.engstruct.2018.05.085.

[30] Toĝan V. Design of planar steel frames using Teaching-Learning Based Optimization. Eng Struct 2012;34:225–32. https://doi.org/10.1016/j.engstruct.2011.08.035.

[31] Kaveh A, Ghazaan MI. Enhanced whale optimization algorithm for sizing optimization of skeletal structures. Mech Based Des Struct Mach 2017;45:345–62. https://doi.org/10.1080/15397734.2016.1213639.